scientific reports

Check for updates

OPEN

Study of β_1-transferrin and β_2-transferrin using microprobe-capture in-emitter elution and high-resolution mass spectrometry

Ruben Yiqi Luo[1,2✉], Christopher Pfaffroth[2], Samuel Yang[1], Kevin Hoang[2], Priscilla S.-W. Yeung[1], James L. Zehnder[1,2] & Run-Zhang Shi[1,2]

Cerebrospinal fluid (CSF) leak can be diagnosed in clinical laboratories by detecting a diagnostic marker β_2-transferrin (β_2-Tf) in secretion samples. β_2-Tf and the typical transferrin (Tf) proteoform in serum, β_1-transferrin (β_1-Tf), are Tf glycoforms. An innovative affinity capture technique for sample preparation, called microprobe-capture in-emitter elution (MPIE), was incorporated with high-resolution mass spectrometry (HR-MS) to study the Tf glycoforms and the primary structures of β_1-Tf and β_2-Tf. To implement MPIE, an analyte is first captured on the surface of a microprobe, and subsequently eluted from the microprobe inside an electrospray emitter. The capture process is monitored in real-time via next-generation biolayer interferometry (BLI). When electrospray is established from the emitter to a mass spectrometer, the analyte is immediately ionized via electrospray ionization (ESI) for HR-MS analysis. Serum, CSF, and secretion samples were analyzed using MPIE-ESI-MS. Based on the MPIE-ESI-MS results, the primary structures of β_1-Tf and β_2-Tf were elucidated. As Tf glycoforms, β_1-Tf and β_2-Tf share the amino acid sequence but contain varying N-glycans: (1) β_1-Tf, the major serum-type Tf, has two G2S2 N-glycans on Asn413 and Asn611; and (2) β_2-Tf, the major brain-type Tf, has an M5 N-glycan on Asn413 and a G0FB N-glycan on Asn611. The resolving power of the innovative MPIE-ESI-MS method was demonstrated in the study of β_2-Tf as well as β_1-Tf. Knowing the N-glycan structures on β_2-Tf allows for the design of more novel test methods for β_2-Tf in the future.

Abbreviations

CSF	Cerebrospinal fluid
Tf	Transferrin
β_1-Tf	β_1-transferrin
β_2-Tf	β_2-transferrin
MPIE	Microprobe-capture in-emitter elution
ESI	Electrospray ionization
HR-MS	High-resolution mass spectrometry
BLI	Biolayer interferometry
IFE	Immunofixation electrophoresis

Cerebrospinal fluid (CSF) leak can occur as a result of laceration, blunt trauma, or surgery. It may lead to potentially life-threatening meningitis if left untreated[1,2]. CSF leak can be diagnosed in clinical laboratories by detecting a diagnostic marker β_2-transferrin (β_2-Tf) in any body fluid—most commonly in rhinorrhea or otorrhea secretion samples. β_2-Tf is a proteoform of human transferrin (Tf) that is mainly present in CSF and barely detectable in other body fluids[3,4]. The clinical utility and diagnostic value of β_2-Tf in CSF leak have been demonstrated[5,6]. β_2-Tf, together with the typical Tf proteoform in serum, β_1-transferrin (β_1-Tf), were named

[1]Department of Pathology, Stanford University, Stanford, CA, USA. [2]Clinical Laboratories, Stanford Health Care, 3375 Hillview Ave, Palo Alto, CA 94304, USA. ✉email: rubenluo@stanford.edu

nature portfolio

1

after their electrophoretic mobility in gel electrophoresis[7]. While β_2-Tf is widely used as a diagnostic marker for CSF leak, the primary structure of β_2-Tf as well as that of β_1-Tf have not been elucidated.

There has been extensive basic research on human Tf since it is a high-abundance protein in blood with a major role in iron metabolism. The amino acid sequence of Tf precursor was determined through protein cleavage and cDNA characterization, showing a full sequence of 698 amino acids; after the removal of an N-terminal signal peptide, the mature form of Tf contains 679 amino acids, 19 intramolecular disulfide bonds formed between cysteine residues, and two N-glycans attached to the amino groups of the side chains of Asn419 and Asn611 (Asn432 and Asn630 of Tf precursor)[8–11]. Tf proteoforms typically vary by the N-glycan structures[11–13], and the Tf proteoforms of interest so far are Tf glycoforms, including β_1-Tf and β_2-Tf[7].

Although it is known that β_2-Tf has desialylated N-glycans while β_1-Tf has fully sialylated N-glycans[3,14,15], the primary structures of β_1-Tf and β_2-Tf have not been clarified. On the other hand, the N-glycans on Tf glycoforms in serum and in CSF were characterized using gel electrophoresis, liquid chromatography, and enzymatic digestion-based mass spectrometry (MS) by neurobiologists[13,16–19]. It was reported that a group of Tf glycoforms were present in serum, namely serum-type Tf glycoforms or sTf, among which a specific Tf glycoform (major serum-type Tf) predominated[12,13]; the serum-type Tf glycoforms also existed in CSF. An additional group of Tf glycoforms were present in CSF, namely brain-type Tf glycoforms, among which a specific Tf glycoform (major brain-type Tf) was more abundant than the rest[15,20]. The brain-type Tf glycoforms was at least partly synthesized in the CSF-producing tissue choroid plexus rather than being produced by glycosidase digestion of serum-type Tf glycoforms[16,20]. It was found that the N-glycans on the major serum-type Tf consisted of bi-antennary oligosaccharide chains with sialylated terminals, and those on the brain-type Tf glycoforms were desialylated, or more specifically, unsialylated (asialotransferrin)[15,16,18,20]. It was hypothesized that the major brain-type Tf was β_2-Tf[21], but this hypothesis has not been proved. Similarly, it is reasonable to presume that the major serum-type Tf was β_1-Tf, however a proof is required.

In clinical cases where CSF leak is suspected, secretion samples can be collected from patients and sent to clinical laboratories to test for the presence of β_2-Tf. The conventional method to test β_2-Tf as well as β_1-Tf is agarose gel immunofixation electrophoresis (IFE)[2–4]. Although it is widely used in clinical laboratories, it does not provide structural information of the analytes. Thus, the primary structures of β_1-Tf and β_2-Tf, particularly the N-glycan structures on these Tf glycoforms, remained an unanswered question with this method.

As an emerging technology in clinical diagnostics, high-resolution mass spectrometry (HR-MS), particularly top-down HR-MS, can be used to analyze a protein target in its intact state and identify the post-translational modifications and amino acid variations in its proteoforms[22–24]. While HR-MS is an ideal tool to study the Tf glycoforms, the quality of data acquired during HR-MS analysis depends on sample preparation[25,26]. In this article, an innovative affinity capture technique for sample preparation, called microprobe-capture in-emitter elution (MPIE), was incorporated with HR-MS to study the Tf glycoforms[27]. MPIE can directly couple a label-free optical sensing technology with MS. The label-free optical sensing technology is next-generation biolayer interferometry (BLI, also named as thin-layer interferometry, TFI), which senses optical thickness changes on the sensing surface of a microprobe caused by biomolecular interactions such as antibody-antigen binding, achieving real-time measurement without employing a reporter molecule (enzyme, fluorophore, etc.)[28,29]. To implement MPIE, an analyte is first captured on the surface of a microprobe, and subsequently eluted from the microprobe inside an electrospray emitter. The capture process is monitored in real-time via BLI. When electrospray is established from the emitter to a mass spectrometer, the analyte is immediately ionized via electrospray ionization (ESI) for HR-MS analysis. By this means, BLI and HR-MS are directly coupled in the form of MPIE-ESI-MS, which is readily deployed to study the Tf glycoforms and the primary structures of β_1-Tf and β_2-Tf.

Methods

Materials and specimens.
LC–MS grade water, acetonitrile, formic acid, and 0.2 µm PVDF syringe filters were purchased from Thermo Fisher Scientific (Waltham, MA). A mouse monoclonal anti-transferrin IgG antibody (anti-Tf Ab) was obtained from Sinobiological (Wayne, PA), and biotinylated using an EZ-Link HPDP-Biotin reagent kit (Waltham, MA). Remnant CSF and serum samples from patients, and secretion samples from patients suspected of CSF leak were obtained from Stanford Health Care and Stanford Children's Health, following an approved institutional review board protocol for the use of remnant patient specimens.

Sample preparation.
The biotinylated anti-Tf Ab was diluted in phosphate-buffered saline at pH 7.4 with 0.02% Tween 20 and 0.2% BSA (PBST-B) to 10 µg/ml for use. A pooled CSF sample was made by mixing 9 CSF samples from patients to explore the analytical sensitivity of MPIE-ESI-MS for β_2-Tf in CSF. The pooled CSF sample was mixed with water to make a dilution series. CSF samples were 1:1 diluted in phosphate-buffered saline at pH 7.4 with 0.02% Tween 20 (PBST) and serum samples were 1:19 diluted in PBST-B. Secretion samples from patients were first mixed with an equal amount of water and filtered using a 0.2 µm PVDF syringe filter, and then 1:1 diluted in PBST.

To study the gel electrophoresis-separated Tf glycoforms, gel electrophoresis of CSF samples was carried out using a Hydragel 6 β_2 Transferrin kit (Sebia, Lisses, France) following the manufacturer's protocol. In brief, a CSF sample was first 1:1 mixed with an iron-saturating solution, and then 10 µl of the sample was loaded to each of the 6 wells on an agarose gel so that replicates were run in all the 6 lanes. Gel electrophoresis was implemented in a Hydrasys 2 instrument (Sebia, Lisses, France), and the agarose gel was removed from the instrument immediately after the gel electrophoresis was completed, without carrying out the immunofixation steps. The agarose gel was placed on a paper template marked with the β_1-Tf and β_2-Tf band regions, and the gel stripes of the band regions were cut out using a scalpel. Each gel stripe was placed in a 1.5 ml sample tube, 200 µl PBST was added, and the sample was rocked for 2 h at room temperature to extract the analyte from the gel stripe. After extraction,

the supernatant was filtered using a 0.2 μm PVDF syringe filter. The images of an agarose gel for MPIE-ESI-MS analysis and a reference agarose gel after immunofixation are posted in Fig. 2.

MPIE-ESI-MS instrumentation and experiment. An MPIE-ESI-MS experiment consists of two parts: BLI-based affinity capture and in-emitter elution ESI-MS, with the details including instrumentation described elsewhere[27]. The BLI-based affinity capture was implemented in a Gator Plus analyzer (Gator Bio, Palo Alto, CA): a BLI microprobe pre-coated with streptavidin was first dipped into the biotinylated anti-Tf Ab solution for 10 min to load the anti-Tf Ab, then dipped into a sample for 10 min to capture Tf molecules, and rinsed in PBST for 1 min to remove non-specifically bound molecules. The in-emitter elution ESI-MS was implemented in an EMASS-II ESI ion source which coupled an ECE-001 capillary electrophoresis instrument (CMP Scientific, Brooklyn, NY) with an Orbitrap Q-Exactive Plus mass spectrometer (Thermo Scientific, San Jose, CA): an electrospray emitter with a regular open end and a tapered open end (tip orifice diameter 20–30 μm) was filled with a sheath liquid (10 mM ammonium formate in water); after affinity capture, the microprobe was rinsed in the sheath liquid for 10 s, inserted into the emitter through the regular open end, and settled in the tapered end by gravity; the emitter was mounted to the ESI ion source, and a capillary was inserted into the emitter through the regular open end and positioned right behind the microprobe to deliver an elution liquid (80% acetonitrile and 2% formic acid in water); once electrospray was established by applying a positive voltage to the sheath liquid in the emitter, HR-MS data acquisition was initiated, and injection of the elution liquid was started subsequently. The emitter was placed ~ 2 mm away from the mass spectrometer inlet with the electrospray voltage set at 2.2 kV. The injection of the elution liquid was driven by 5 psi pneumatic pressure. The following MS parameters were used: ion-transfer capillary temperature 350 °C, S-lens RF level 50, and number of microscans 10. Primary mass spectra were acquired in positive polarity at resolution 17.5 K.

Data analysis. In HR-MS analysis of proteins, it is necessary to deconvolute raw MS data to merge the multiple charge states and isotopic peaks of an analyte to obtain its accurate molecular mass. The acquired data in each MPIE-ESI-MS experiment was viewed as a time trace of MS responses, and the elution time window of an analyte was identified by checking the molecular ions of the analyte at each time point. The data in the elution time window were selected for deconvolution using Biopharma Finder 4.1 (Thermo Fisher Scientific, San Jose, CA) with the ReSpect algorithm. MS peaks of analytes were displayed in deconvoluted mass spectra at uncharged state showing average molecular masses.

Ethics approval. Informed consent was not required because only remnant clinical samples were used in this study. An institutional review board approval (Protocol 66,075 by Panel on Medical Human Subjects of Stanford University) for the use of remnant patient specimens was obtained. All methods were carried out in accordance with relevant guidelines and regulations.

Results

The performance of MPIE-ESI-MS for Tf analysis was demonstrated and reported elsewhere[27]. MPIE-ESI-MS had a limit of detection for the Tf standard at 0.063 μg/ml, which was translated to no more than 7 fmol Tf molecules captured on a microprobe[27]. The high analytical sensitivity and specificity provided by affinity capture made MPIE-ESI-MS an ideal method to study the Tf molecules. The results of a set of serum, CSF, and secretion samples are shown in Fig. 1. The deconvoluted mass spectrum of the serum sample showed a group of MS peaks around 79,554 Da; they are mainly serum-type Tf glycoforms and the predominant MS peak at 79,554 Da is the major serum-type Tf (N-glycan structures shown in Fig. 1, see details in Discussion). The deconvoluted mass spectrum of the CSF sample showed the major serum-type Tf and a group of MS peaks around 78,008 Da; they are mainly brain-type Tf glycoforms and the most abundant MS peak at 78,008 Da is the major brain-type Tf (N-glycan structures shown in Fig. 1, see details in Discussion). The deconvoluted mass spectrum of the secretion sample showed both serum-type and brain-type Tf glycoforms, meaning that CSF was present in the sample. This finding was consistent with the fact that the secretion sample was obtained from a patient diagnosed with CSF leak. In addition, the BLI sensorgrams (a time trace of label-free optical sensing responses) during the capture of Tf as well as the BLI sensorgrams of negative controls (PBST-B and PBST) are shown in Supplementary Figure S1. The BLI measurement facilitates real-time monitoring of the capture process.

To figure out the relationship between the major serum-type Tf, the major brain-type Tf and β_1-Tf, β_2-Tf, after gel electrophoresis of CSF samples, the extracts from the gel stripes of the β_1-Tf and β_2-Tf band regions were analyzed using MPIE-ESI-MS. The results of a CSF sample are shown in Fig. 2. The deconvoluted mass spectra showed only the MS peak of the major serum-type Tf in the extract from the β_1-Tf band region and only the MS peak of the major brain-type Tf in the extract from the β_2-Tf band region. The measured accurate molecular masses were consistent with the experiments in Fig. 1 and matched the theoretical molecular masses of the major serum-type Tf and major brain-type Tf (N-glycan structures shown in Fig. 2, see details in Discussion). This observation proved the hypothesis that β_1-Tf and β_2-Tf were actually the major serum-type Tf and major brain-type Tf, respectively. In addition, the gel area between the β_1-Tf and β_2-Tf band regions was also analyzed and minor Tf glycoforms in serum and CSF were not found, which could be due to the low quantities of the minor Tf glycoforms in a gel stripe.

A collection of 11 secretion samples from patients suspected of CSF leak were analyzed using the MPIE-ESI-MS method, among which 5 samples were positive for β_2-Tf and the rest were negative as measured by the conventional IFE test. As shown in Table 1, the MS peak at 78,008 Da was observed in the MPIE-ESI-MS results of the 5 positive samples but not found in those of the 6 negative samples, which confirmed the consistency between the MPIE-ESI-MS method and the conventional IFE test. In addition, the limit of detection of the MPIE-ESI-MS
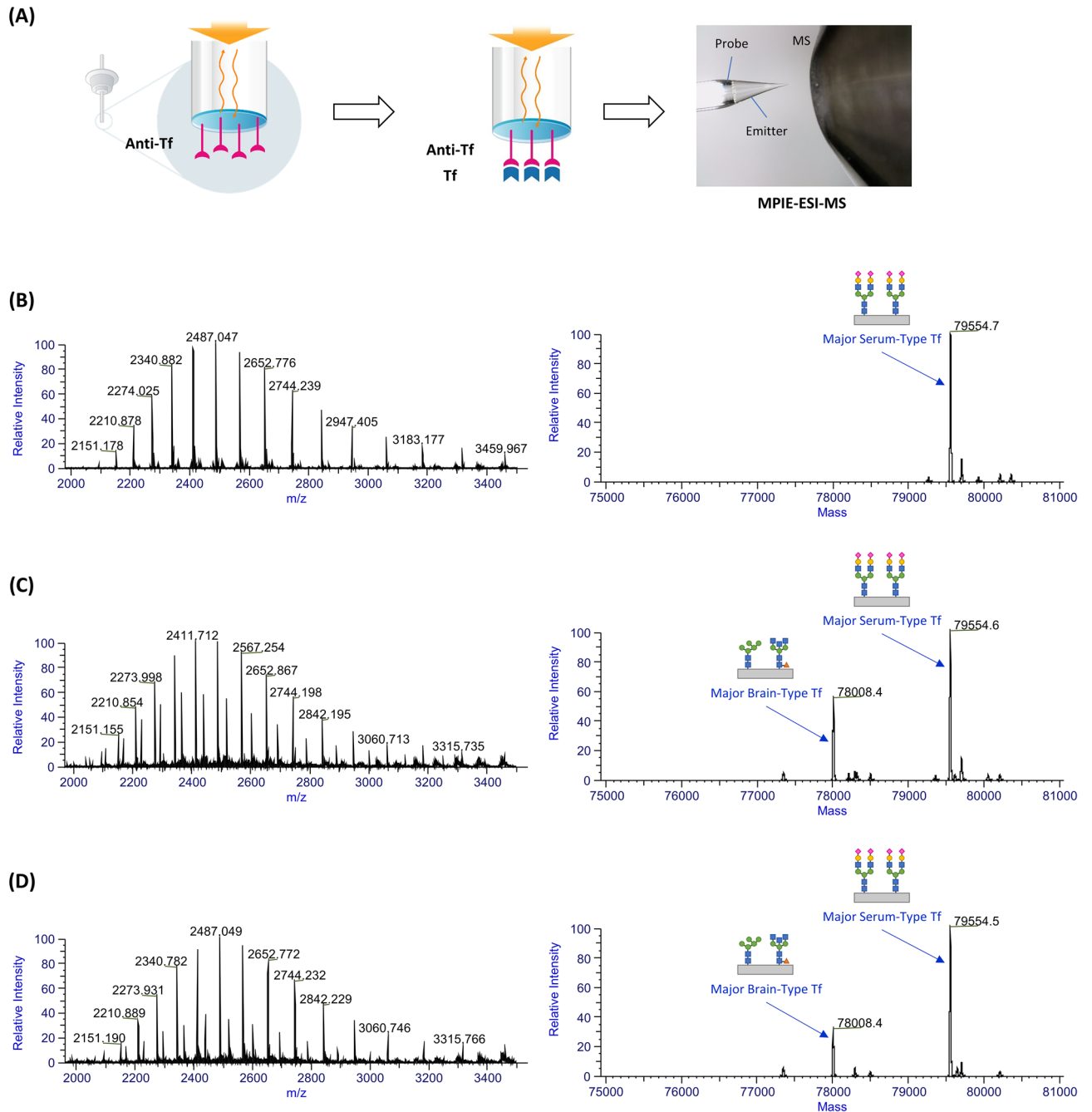
Figure 1. (**A**) Experiment workflow of MPIE-ESI-MS for Tf analysis. The MPIE-ESI-MS results of (**B**) a serum sample, (**C**) a CSF sample, and (**D**) a secretion sample from a patient diagnosed of CSF leak: HR-MS raw mass spectra (left) and deconvoluted mass spectra (right) of captured Tf molecules, showing serum-type Tf glycoforms in (**B**), and both serum-type Tf and brain-type Tf glycoforms in (**C**) and (**D**).

method was explored. A pooled CSF sample was mixed with water at 1:1, 1:4, 1:9, and 1:19 ratios to prepare a dilution series for analysis. Supplementary Table S1 summarizes the results, listing the MS peak intensities of β_1-Tf and β_2-Tf in the deconvoluted mass spectra (the entire time window of Tf elution selected for deconvolution). The peak intensities decreased with the pooled CSF sample dilution, and it was demonstrated that the MPIE-ESI-MS method was able to detect β_2-Tf in at least tenfold diluted CSF (1:9 pooled CSF: water mixture).

Discussion

The MPIE-ESI-MS analysis of the extracts from the gel stripes proved that β_1-Tf and β_2-Tf were identical to the major serum-type Tf and the major brain-type Tf, respectively. As Tf glycoforms, β_1-Tf and β_2-Tf share the amino acid backbone but contain varying N-glycans. The amino acid sequence of Tf was previously investigated and reported[8,9]. The primary structure of a mature Tf molecule is composed of 679 amino acids with
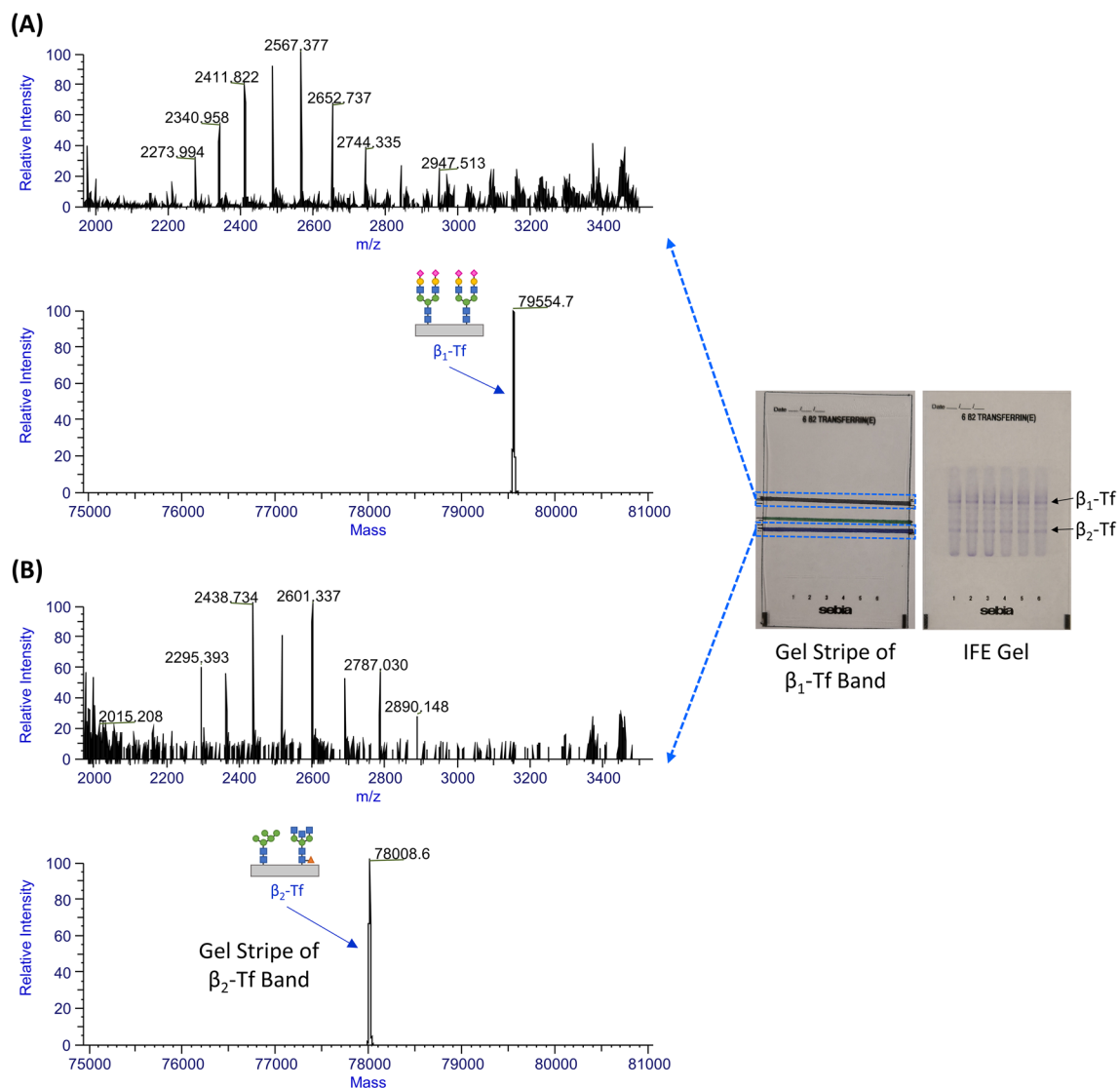
Figure 2. The MPIE-ESI-MS results of (**A**) the extract from the gel stripe of the β_1-Tf band region and (**B**) the extract from the gel stripe of the β_2-Tf band region: HR-MS raw mass spectra (left) and deconvoluted mass spectra (right) of captured Tf molecules, showing β_1-Tf in (**A**) and β_2-Tf in (**B**). The image of an agarose gel after gel electrophoresis is posted to the right of the mass spectra, which was placed on the paper template marked with the β_1-Tf and β_2-Tf band regions. The image of a reference agarose gel after immunofixation is posted further on the right, indicating the β_1-Tf and β_2-Tf band regions designated according to the manufacturer's protocol.

Secretion sample	β1-Tf		β2-Tf	
	Detected?	Measured molecular mass	Detected?	Measured molecular mass
Positive sample 1	Yes	79,554.50 Da	Yes	78,008.42 Da
Positive sample 2	Yes	79,554.79 Da	Yes	78,008.60 Da
Positive sample 3	Yes	79,554.75 Da	Yes	78,008.83 Da
Positive sample 4	Yes	79,554.04 Da	Yes	78,008.68 Da
Positive sample 5	Yes	79,554.77 Da	Yes	78,008.03 Da
Negative sample 1	Yes	79,554.29 Da	No	/
Negative sample 2	Yes	79,554.80 Da	No	/
Negative sample 3	Yes	79,554.81 Da	No	/
Negative sample 4	No	/	No	/
Negative sample 5	Yes	79,554.49 Da	No	/
Negative sample 6	Yes	79,554.73 Da	No	/

Table 1. The MPIE-ESI-MS results of 11 secretion samples from patients suspected of CSF leak.
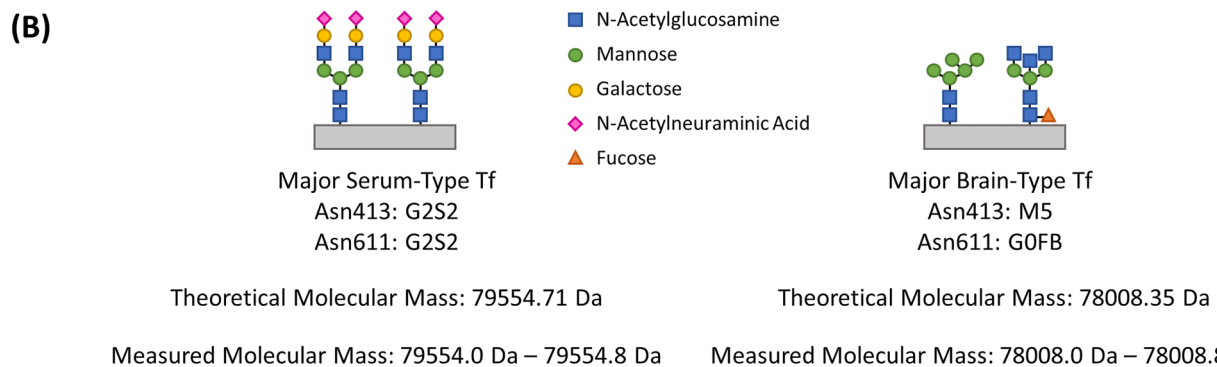
19 disulfide bonds and 2 N-glycans, as illustrated in Fig. 3A. N-glycans on proteins typically include bi-, tri-, or tetra-antennary oligosaccharide chains resulted from sequential action of glycosyltransferases[30,31], and an N-glycan can be named according to its sugar composition and branching structure (traditional nomenclature used in this article)[32]. When the potential varieties of N-glycans are established, the structures of Tf glycoforms can be confirmed by aligning the measured accurate molecular masses with the theoretical molecular masses of the potential Tf glycoforms.

The potential structures of N-glycans on Tf were previously reported by employing enzymatic digestion-based MS analysis of the Tf glycoforms in CSF[17,19]. It was revealed that the most abundant N-glycan type was G2S2. Quantitation of the digested glycopeptides encompassing the glycosylation sites found that G2S2 consisted of roughly 65% of all N-glycans on Asn413 and 73% of all N-glycans on Asn611[17]. Thus, the Tf glycoform with two G2S2 N-glycans on Asn413 and Asn611 aligns with β_1-Tf for the following reasons: (1) the measured molecular mass of β_1-Tf exactly matches its theoretical molecular mass 79,554.71 Da (Fig. 3B), (2) it is the most abundant Tf glycoform in serum and CSF, and (3) it is consistent with the fact that β_1-Tf is fully sialylated (N-acetylneuraminic acid as the sialic acid). In addition, the Tf glycoforms associated with M5 and G0FB N-glycans must be the most abundant unsialylated Tf glycoforms in CSF provided that the two N-glycans were found to be the most abundant unsialylated N-glycans[19]. Particularly, M5 was found consisting of roughly 20% of all N-glycans on Asn413 and G0FB was found consisting of 26% of all N-glycans on Asn611[17]. Among the possible combinations of the two N-glycans, the Tf glycoform with an M5 N-glycan and a G0FB N-glycan matches β_2-Tf because (1) the measured molecular mass of β_2-Tf exactly matches its theoretical molecular mass 78,008.35 Da (Fig. 3B), and (2) it is consistent with the fact that β_2-Tf is unsialylated. The glycosylation sites of the M5 and G0FB N-glycans were found to be on Asn413 and Asn611 respectively by another study of digested glycopeptides from Tf glycoforms in CSF[18]. The presence of a bisecting N-acetylglucosamine (GlcNAc) in the G0FB N-glycan was proved by the previously reported lectin-binding experiments[16], verifying the structure of G0FB N-glycan over another possible isomeric N-glycan without a bisecting GlcNAc[19]. Thus, the analysis above substantiates the following findings: (1) β_1-Tf, the major serum-type Tf, has two G2S2 N-glycans on Asn413 and Asn611; and (2) β_2-Tf, the major brain-type Tf, has an M5 N-glycan on Asn413 and a G0FB N-glycan on Asn611.

Besides the two major Tf glycoforms in CSF (β_1-Tf and β_2-Tf), it is known that other minor Tf glycoforms may also exist in CSF, blood, and other body fluids[4,33]. As illustrated in the previous literature, there are a variety of unsialylated N-glycans on Tf molecules, and the sialylated N-glycan G2S2 also has diversity such as the more branched form G3S3[13,17,34]. Thus, a number of fully sialylated, partially sialylated, and unsialylated Tf glycoforms can be formed by the various combinations of the two N-glycans on a Tf molecule. In gel electrophoresis, sialic acids bring negative charges to a Tf molecule under neutral or alkaline pH conditions, influencing its electrophoretic mobility. As such, Tf glycoforms migrate in the order of fully sialylated, disialylated, and unsialylated Tf glycoforms, with regard to the number of sialic acids on the N-glycans. Thus, the minor Tf glycoforms can migrate within or between the β_1-Tf and β_2-Tf band regions. For instance, the product insert of the Hydragel 6

(A)

VPDKTVRWCA VSEHEATKCQ SFRDHMKSVI PSDGPSVACV KKASYLDCIR AIAANEADAV TLDAGLVYDA YLAPNNLKPV VAEFYGSKED
PQTFYYAVAV VKKDSGFQMN QLRGKKSCHT GLGRSAGWNI PIGLLYCDLP EPRKPLEKAV ANFFSGSCAP CADGTDFPQL CQLCPGCGCS
TLNQYFGYSG AFKCLKDGAG DVAFVKHSTI FENLANKADR DQYELLCLDN TRKPVDEYKD CHLAQVPSHT VVARSMGGKE DLIWELLNQA
QEHFGKDKSK EFQLFSSPHG KDLLFKDSAH GFLKVPPRMD AKMYLGYEYV TAIRNLREGT CPEAPTDECK PVKWCALSHH ERLKCDEWSV
NSVGKIECVS AETTEDCIAK IMNGEADAMS LDGGFVYIAG KCGLVPVLAE NYNKSDNCED TPEAGYFAVA VVKKSASDLT WDNLKGKKSC
HTAVGRTAGW NIPMGLLYNK INHCRFDEFF SEGCAPGSKK DSSLCKLCMG SGLNLCEPNN KEGYYGYTGA FRCLVEKGDV AFVKHQTVPQ
NTGGKNPDPW AKNLNEKDYE LLCLDGTRKP VEEYANCHLA RAPNHAVVTR KDKEACVHKI LRQQQHLFGS NVTDCSGNFC LFRSETKDLL
FRDDTVCLAK LHDRNTYEKY LGEEYVKAVG NLRKCSTSSL LEACTFRRP

Primary Structure of Human Transferrin: 679 AA, 19 Disulfide Bonds (Orange Label), 2 N-Glycosylation Sites (Blue Label)

(B)

Major Serum-Type Tf
Asn413: G2S2
Asn611: G2S2

Major Brain-Type Tf
Asn413: M5
Asn611: G0FB

Theoretical Molecular Mass: 79554.71 Da

Theoretical Molecular Mass: 78008.35 Da

Measured Molecular Mass: 79554.0 Da – 79554.8 Da

Measured Molecular Mass: 78008.0 Da – 78008.8 Da

Figure 3. (**A**) Primary structure of human transferrin, showing the sequence of 679 amino acids, 19 disulfide bonds, and 2 N-glycosylation sites. (**B**) N-glycan structures on β_1-Tf (major serum-type Tf) and β_2-Tf (major brain-type Tf), confirmed by comparing the theoretical molecular masses of the Tf glycoforms with the measured molecular masses in Figs. 1, 2, and Table 1.

β_2 Transferrin kit states that a band of disialylated Tf glycoforms (disialotransferrin) may exist above the β_2-Tf band[35]. On the other hand, the unsialylated Tf glycoforms besides β_2-Tf can migrate within the β_2-Tf band region and interfere with the β_2-Tf detection. The product insert suggests to use the ratio of unsialylated to disialylated bands to confirm the presence of β_2-Tf. The reason of this practice can be explained as follows: when CSF is present in a sample, the abundance of the major unsialylated Tf glycoform β_2-Tf significantly exceeds the minor unsialylated and disialylated Tf glycoforms, resulting in a high ratio of the β_2-Tf band to the disialotransferrin band. This practice in the IFE test can be achieved in the MPIE-ESI-MS analysis as all the Tf glycoforms are shown in a deconvoluted mass spectrum and the MS peak intensities represent their relative quantities. However, it is probably unnecessary because β_2-Tf can be specifically detected by its accurate molecular mass and definitively differentiated from other unsialylated and disialylated Tf glycoforms.

The demonstration of MPIE-ESI-MS in detection of β_2-Tf paved a way to establish an MS-based clinical assay for β_2-Tf. When implementing the accurate molecular mass-based detection of β_2-Tf, Tf variants resulted from genetic polymorphism should be taken into consideration[11,36–39]. In theory, amino acid variation in the Tf molecule can change the molecular masses of β_1-Tf and β_2-Tf but not the molecular mass difference between the two Tf glycoforms (1546 Da), provided the two glycosylation sites are not modified. This hypothesis is supported by the MPIE-ESI-MS results of a few Tf variant-containing CSF samples, as shown in Supplementary Figure S2A and S2B. In addition, the N-glycans on serum-type Tf glycoforms can vary under specific pathophysiological conditions such as carbohydrate-deficient syndromes and alcohol abuse. β_1-Tf might not be found in those samples due to aberrant glycosylation[12,34,40–42]. As an example, Supplementary Figure S2C shows altered Tf glycoforms in a CSF sample from an alcohol-consuming patient. These topics are beyond the scope of this article and can be investigated in the future when an MS-based clinical assay for β_2-Tf is being developed.

As an innovative affinity capture technique, MPIE facilitates real-time monitoring of the affinity capture process to overcome the lack of process monitoring in conventional affinity capture techniques. The assembly of a BLI microprobe and an electrospray emitter restricts dispersion of eluted analyte in MPIE-ESI-MS and substantially brings up the concentration of the minute amount of analyte captured by a BLI microprobe, allowing for good analytical sensitivity. Currently MPIE-ESI-MS is not an ideal tool for quantitative analysis due to the variation in capture agent loading and analyte binding on a BLI microprobe, as well as that in MS ionization. In the future, when accurate quantitation is needed, quantitative MPIE-ESI-MS analysis should be achievable by employing internal standards, i.e., preferably stable isotope-labeled analytes[27].

Conclusions

The resolving power of the innovative MPIE-ESI-MS method was demonstrated in the study of β_2-Tf as well as β_1-Tf. Knowing the N-glycan structures on β_2-Tf allows for the design of more novel test methods for β_2-Tf in the future. For instance, it is possible to employ specific carbohydrate-binding lectins to selectively capture β_2-Tf for MS analysis or lectin-antibody assays.

Data availability

All data generated or analyzed during this study are included in this published article and its supplementary information.

References

1. Warnecke, A. *et al.* Diagnostic relevance of β2-transferrin for the detection of cerebrospinal fluid fistulas. *Arch. Otolaryngol. Neck Surg.* **130**(10), 1178. https://doi.org/10.1001/archotol.130.10.1178 (2004).
2. McCudden, C. R. *et al.* Evaluation of high resolution gel β2-transferrin for detection of cerebrospinal fluid leak. *Clin. Chem. Lab. Med. CCLM* **51**(2), 311–315. https://doi.org/10.1515/cclm-2012-0408 (2013).
3. Papadea, C. & Schlosser, R. J. Rapid method for β2-transferrin in cerebrospinal fluid leakage using an automated immunofixation electrophoresis system. *Clin. Chem.* **51**(2), 464–470. https://doi.org/10.1373/clinchem.2004.042697 (2005).
4. Görögh, T. *et al.* Separation of β2-transferrin by denaturing gel electrophoresis to detect cerebrospinal fluid in ear and nasal fluids. *Clin. Chem.* **51**(9), 1704–1710. https://doi.org/10.1373/clinchem.2005.054916 (2005).
5. Zaret, D. L., Morrison, N., Gulbranson, R. & Keren, D. F. Immunofixation to quantify β2-transferrin in cerebrospinal fluid to detect leakage of cerebrospinal fluid from skull injury. *Clin. Chem.* **38**(9), 1909–1912. https://doi.org/10.1093/clinchem/38.9.1909 (1992).
6. Nandapalan, V., Watson, I. D. & Swift, A. C. Beta-2-transferrin and cerebrospinal fluid rhinorrhoea. *Clin. Otolaryngol.* **21**(3), 259–264. https://doi.org/10.1111/j.1365-2273.1996.tb01737.x (1996).
7. Gallo, P., Bracco, F., Morara, S., Battistin, L. & Tavolato, B. The cerebrospinal fluid transferrin/Tau proteins. *J. Neurol. Sci.* **70**(1), 81–92. https://doi.org/10.1016/0022-510X(85)90190-X (1985).
8. Yang, F. *et al.* Human transferrin: cDNA characterization and chromosomal localization. *Proc. Natl. Acad. Sci.* **81**(9), 2752–2756. https://doi.org/10.1073/pnas.81.9.2752 (1984).
9. MacGillivray, R. T. *et al.* The complete amino acid sequence of human serum transferrin. *Proc. Natl. Acad. Sci.* **79**(8), 2504–2508. https://doi.org/10.1073/pnas.79.8.2504 (1982).
10. Wang, S. & Kaltashov, I. A. Identification of reduction-susceptible disulfide bonds in transferrin by differential alkylation using O^{16}/O^{18} labeled iodoacetic acid. *J. Am. Soc. Mass Spectrom.* **26**(5), 800–807. https://doi.org/10.1007/s13361-015-1082-5 (2015).
11. de Jong, G., van Dijk, J. P. & van Eijk, H. G. The biology of transferrin. *Clin. Chim. Acta* **190**(1–2), 1–46. https://doi.org/10.1016/0009-8981(90)90278-Z (1990).
12. de Jong, G. & van Eijk, H. G. Microheterogeneity of human serum transferrin: A biological phenomenon studied by isoelectric focusing in immobilized pH gradients. *Electrophoresis* **9**(9), 589–598. https://doi.org/10.1002/elps.1150090921 (1988).
13. de Jong, G., van Noort, W. L. & van Eijk, H. G. Carbohydrate analysis of transferrin subfractions isolated by preparative isoelectric focusing in immobilized pH gradients. *Electrophoresis* **13**(1), 225–228. https://doi.org/10.1002/elps.1150130146 (1992).
14. Delaroche, O., Bordureb, P., Lippert, E. & Sagnieza, M. Perilymph detection by β2-transferrin immunoblotting assay. Application to the diagnosis of perilymphatic fistulae. *Clin. Chim. Acta* **245**(1), 93–104. https://doi.org/10.1016/0009-8981(95)06177-0 (1996).

15. Hoffmann, A., Nimtz, M., Getzlaff, R. & Conradt, H. S. 'Brain-type' *N*-glycosylation of asialo-transferrin from human cerebrospinal fluid. *FEBS Lett.* **359**(2–3), 164–168. https://doi.org/10.1016/0014-5793(95)00034-7 (1995).

16. Futakawa, S. *et al.* A unique N-glycan on human transferrin in CSF: A possible biomarker for iNPH. *Neurobiol. Aging* **33**(8), 1807–1815. https://doi.org/10.1016/j.neurobiolaging.2011.02.023 (2012).

17. Brown, K. J., Vanderver, A., Hoffman, E. P., Schiffmann, R. & Hathout, Y. Characterization of transferrin glycopeptide structures in human cerebrospinal fluid. *Int. J. Mass Spectrom.* **312**, 97–106. https://doi.org/10.1016/j.ijms.2011.06.021 (2012).

18. Nagae, M. *et al.* Structural change of N-glycan exposes hydrophobic surface of human transferrin. *Glycobiology* **24**(8), 693–702. https://doi.org/10.1093/glycob/cwu033 (2014).

19. Hoshi, K. *et al.* Transferrin biosynthesized in the brain is a novel biomarker for Alzheimer's disease. *Metabolites* **11**(9), 616. https://doi.org/10.3390/metabo11090616 (2021).

20. Hoshi, K. *et al.* A unique glycan-isoform of transferrin in cerebrospinal fluid: A potential diagnostic marker for neurological diseases. *Biochim. Biophys. Acta BBA – Gen. Subj.* **1861**(10), 2473–2478. https://doi.org/10.1016/j.bbagen.2017.07.005 (2017).

21. Caslavska, J., Schild, C. & Thormann, W. High-resolution capillary zone electrophoresis and mass spectrometry for distinction of undersialylated and hypoglycosylated transferrin glycoforms in body fluids. *J. Sep. Sci.* **43**(1), 241–257. https://doi.org/10.1002/jssc.201900857 (2020).

22. Siuti, N. & Kelleher, N. L. Decoding protein modifications using top-down mass spectrometry. *Nat. Methods* **4**(10), 817–821. https://doi.org/10.1038/nmeth1097 (2007).

23. Brown, K. A., Melby, J. A., Roberts, D. S. & Ge, Y. Top-down proteomics: Challenges, innovations, and applications in basic and clinical research. *Expert Rev. Proteomics* **17**(10), 719–733. https://doi.org/10.1080/14789450.2020.1855982 (2020).

24. Luo, R. Y. *et al.* Neutral-coating capillary electrophoresis coupled with high-resolution mass spectrometry for top-down identification of hemoglobin variants. *Clin. Chem.* https://doi.org/10.1093/clinchem/hvac171 (2022).

25. Donnelly, D. P. *et al.* Best practices and benchmarks for intact protein analysis for top-down mass spectrometry. *Nat. Methods* **16**(7), 587–594. https://doi.org/10.1038/s41592-019-0457-0 (2019).

26. Padula, M. *et al.* A comprehensive guide for performing sample preparation and top-down protein analysis. *Proteomes* **5**(4), 11. https://doi.org/10.3390/proteomes5020011 (2017).

27. Luo, R. Y. & Yang, S. Microprobe-capture in-emitter elution: An affinity capture technique to directly couple a label-free optical sensing technology with mass spectrometry for protein analysis. *Anal. Chem.* **95**(13), 5494–5499. https://doi.org/10.1021/acs.analchem.2c04727 (2023).

28. Luo, Y. R., Chakraborty, I., Lazar-Molnar, E., Wu, A. H. B. & Lynch, K. L. Development of label-free immunoassays as novel solutions for the measurement of monoclonal antibody drugs and antidrug antibodies. *Clin. Chem.* **66**(10), 1319–1328. https://doi.org/10.1093/clinchem/hvaa179 (2020).

29. Luo, Y. R., Yun, C., Chakraborty, I., Wu, A. H. B. & Lynch, K. L. A SARS-CoV-2 label-free surrogate virus neutralization test and a longitudinal study of antibody characteristics in COVID-19 patients. *J. Clin. Microbiol.* https://doi.org/10.1128/JCM.00193-21 (2021).

30. Bieberich, E. Synthesis, processing, and function of N-glycans in N-glycoproteins. In *Glycobiology of the Nervous System* Vol. 9 (eds Yu, R. K. & Schengrund, C. L.) 47–70 (Advances in Neurobiology Springer, 2014). https://doi.org/10.1007/978-1-4939-1154-7_3.

31. Cao, L. *et al.* Global site-specific analysis of glycoprotein N-glycan processing. *Nat. Protoc.* **13**(6), 1196–1212. https://doi.org/10.1038/nprot.2018.024 (2018).

32. Maier, M. *et al.* Applying mini-bore HPAEC-MS/MS for the characterization and quantification of Fc N-glycans from heterogeneously glycosylated IgGs. *J. Chromatogr. B* **1033–1034**, 342–352. https://doi.org/10.1016/j.jchromb.2016.08.001 (2016).

33. Kleinert, P. *et al.* Mass spectrometric analysis of human transferrin in different body fluids. *Clin. Chem. Lab. Med.* https://doi.org/10.1515/CCLM.2003.241 (2003).

34. Coddeville, B., Carchon, H., Jaeken, J., Briand, G. & Spik, G. Determination of glycan structures and molecular masses of the glycovariants of serum transferrin from a patient with carbohydrate deficient syndrome type II. *Glycoconj. J.* **15**(3), 265–273. https://doi.org/10.1023/A:1006997012617 (1998).

35. HYDRAGEL 6 ß2 TRANSFERRIN(E) Kit Instruction Manual. Published online March (2011).

36. Caslavska, J., Lanz, C., Burda, P., Tobler, M. & Thormann, W. Analysis of genetic variants of transferrin in human serum after desialylation by capillary zone electrophoresis and capillary isoelectric focusing. *J. Sep. Sci.* **40**(11), 2488–2497. https://doi.org/10.1002/jssc.201700211 (2017).

37. Lee, P. L., Halloran, C., Trevino, R., Felitti, V. & Beutler, E. Human transferrin G277S mutation: A risk factor for iron deficiency anaemia: Transferrin G277S mutation and anaemia. *Br. J. Haematol.* **115**(2), 329–333. https://doi.org/10.1046/j.1365-2141.2001.03096.x (2001).

38. Pang, H., Koda, Y., Soejima, M. & Kimura, H. Identification of a mutation (A1879G) of transferrin from cDNA prepared from peripheral blood cells. *Ann. Hum. Genet.* **62**(3), 271–274. https://doi.org/10.1046/j.1469-1809.1998.6230271.x (1998).

39. Evans, R. W. *et al.* Characterization and structural analysis of a functional human serum transferrin variant and implications for receptor recognition. *Biochemistry* **33**(41), 12512–12520. https://doi.org/10.1021/bi00207a019 (1994).

40. Arndt, T. Carbohydrate-deficient transferrin as a marker of chronic alcohol abuse: A critical review of preanalysis, analysis, and interpretation. *Clin. Chem.* **47**(1), 13–27 (2001).

41. Helander, A., Eriksson, G., Stibler, H. & Jeppsson, J. O. Interference of transferrin isoform types with carbohydrate-deficient transferrin quantification in the identification of alcohol abuse. *Clin. Chem.* **47**(7), 1225–1233 (2001).

42. Helander, A. *et al.* Reprint of standardisation and use of the alcohol biomarker carbohydrate-deficient transferrin (CDT). *Clin. Chim. Acta* **467**, 15–20. https://doi.org/10.1016/j.cca.2017.03.018 (2017).

Acknowledgements

Author contributions

R.Y.L. contributed to conceptualization, methodology, investigation, resources, data curation, visualization, writing—original draft, writing—review and editing, and project administration of this research; C.P. contributed to investigation and resources of this research; S.Y., K.H., and J.L.Z. contributed to resources of this research; P.S.Y. contributed to writing—review and editing of this research; R.Z. contributed to conceptualization, data curation, writing—review and editing of this research.

Competing interests

Samuel Yang is also an employee of Gator Bio, which is the manufacturer of the Gator Plus analyzer used in this research. The other authors have no competing interest to declare.

Additional information

Supplementary Information The online version contains supplementary material available at https://doi.org/10.1038/s41598-023-42064-7.

Correspondence and requests for materials should be addressed to R.Y.L.

Reprints and permissions information is available at www.nature.com/reprints.

Publisher's note Springer Nature remains neutral with regard to jurisdictional claims in published maps and institutional affiliations.